Romanian Reports in Physics, Vol. 64, No. 3, P. 788–794, 2012

EUROPIUM DOPED HYDROXYAPATITE FOR APPLICATIONS IN ENVIRONMENTAL FIELD*

L.V. CONSTANTIN[1], S. ICONARU[2], C.S. CIOBANU[2*]

[1]University of Bucharest, Faculty of Physics, P.O. Box MG-11, Bucharest, Romania, E-mail: liliana2009constantin@yahoo.com or constantin.liliana@gmail.com

[2]National Institute of Materials Physics, P.O. Box MG-7, Bucharest-Măgurele, Ilfov, 077125, Romania, E-mail: ciobanu_carmen83@yahoo.com

Received July 29, 2011

Abstract. Due to the extensive use of new technologies in agricultural and industrial field the soil and groundwater were severely polluted with elements that may pose a serious threat to the environment. For that purpose studies concerning new materials that can be successfully used for removal of heavy metals and other toxic elements from contaminated soil and water were conducted. The attention of the scientific studies were focused on the family of calcium phosphates, with a particular interest in hydroxyapatite (HAp), with general formula $Ca_{10}(PO_4)_6(OH)_2$, due to the exquisite ability of adsorbing heavy element ions in aqueous conditions. This study focuses on synthesizing nanocrystalline hydroxyapatite powders with controllable parameters and very good stoechiometry. The structure, morphology and optical properties were characterized by X-ray diffraction (XRD), transmission electron microscopy (TEM), scanning electron microscopy (SEM), X-ray photoelectron spectroscopy (XPS), and Fourier transform infrared spectroscopy (FT-IR).

Key words: hydroxyapatite, europium.

1. INTRODUCTION

The presence of big amounts of heavy metals and other toxic elements in the water stream, soil and atmosphere has become of great importance due to their harmful effect to the environment and human health. Even low concentration of heavy metals can have a serious impact on the environment quality and human health [1–3]. Nowadays, numerous methods such as: oxidation, reduction, precipitation, membrane filtration, ion exchange, electrochemical operation, biological treatment [4-6], adsorbtion, have been considered and implemented for removal of heavy metals from wastewaters or soil [7–9]. The most suitable process for removal heavy metals from solutions proved to be adsorption onto solid

* Paper presented at the Annual Scientific Session of Faculty of Physics, University of Bucharest, June 17, 2011, Bucharest-Magurele, Romania.

substrate materials. Working towards developing new materials able to adsorb heavy element encountered difficulties due to high costs of obtaining and implementing them. The solution for achieving high performance at a low cost was found in using as a sorbent of heavy metals hydroxyapatite.

Hydroxyapatite (HAp) is the major inorganic component of bone and dental enamel and is found in the human body. Synthetic HAp nanoparticles are similar to the natural bone and it is broadly used as bone substitute or dental enamel remineralisation material for its excellent bioactivity, biocompatibility, and osteo-conductivity. Hydroxyapatite, $Ca_{10}(PO_4)_6(OH)_2$ has a hexagonal structure with P63/m space group and cell dimensions of $a = b = 9.42$ Å and $c = 6.88$ Å. Because of the high stability and flexibility of the apatite structure, a great number of substitutions, especially the composites resulting from the cationic substitution are of potential application in the fields of dental and bone pathologies, bio ceramics, luminescence [10–14], water purification and catalysis [15–21]. The sorption properties of HAp are of great importance to the environmental applications and to the industrial field.

2. EXPERIMENTAL

2.1. SAMPLE PREPARATION

All the reagents for synthesis including ammonium dihydrogen phosphate [$(NH_4)_2HPO_4$], calcium nitrate [$Ca(NO_3)_2{\cdot}4H_2O$], and europium nitrate [$Eu(NO_3)_3{\cdot}6H_2O$] (Alpha Aesare) were purchased without further purification.

Europium doped hydroxyapatite (EuHAp) nanoparticles was performed by setting the atomic ratio of Eu/[Eu + Ca] at 20% (HAp_Eu20) and [Ca+Eu]/P as 1.67. The $Eu(NO_3)_3{\cdot}6H_2O$ and $Ca(NO_3)_2{\cdot}4H_2O$ were dissolved in deionised water to obtain [Ca+Eu]-containing solution. On the other hand the $(NH_4)_2HPO_4$ was dissolved in deionised water to make P-containing solution. The [Ca+Eu]-containing solution was put into a Berzelius and heated to the temperature of 80^0C and stirred continually 30'. Meanwhile the pH of P-containing solution was adjusted to 9 with NH_3 and stirred continually 30'. The P-containing solution was added drop by drop into the [Ca+Eu]-containing solution and stirred continually 2h and the pH was constantly adjusted and kept at 10 during the reaction. After the reaction the deposited mixtures were washed several times with deionised water. The resulting material was dried at 50^0C for 72h.

2.2. SAMPLE CHARACTERIZATION

X-ray diffraction (XRD). The samples were characterized for phase content by X-ray diffraction (XRD) with a Bruker D8-Advance X-ray diffractometer in the scanning range $2\theta = 20–70$ using CuKα1 incident radiation.

Transmission electron microscopy (TEM) studies were carried out using a JEOL 200 CX. The specimen for TEM imaging was prepared from the particles suspension in deionised water. A drop of well-dispersed supernatant was placed on a carbon – coated 200 mesh copper grid, followed by drying the sample at ambient conditions before it is attached to the sample holder on the microscope.

Scanning electron microscopy (SEM). The structure and morphology of the samples were studied using a HITACHI S2600N-type scanning electron microscope (SEM), operating at 25kV in vacuum. The SEM studies were performed on powder samples. For the elemental analysis the electron microscope was equipped with an energy dispersive X-ray attachment (EDAX/2001 device).

FT-IR spectroscopy. The functional groups present in the prepared powder and in the powders calcined at different temperatures were identified by FTIR (Spectrum BX Spectrometer). For this 1% of the powder was mixed and ground with 99% KBr. Tablets of 10 mm diameter for FTIR measurements were prepared by pressing the powder mixture at a load of 5 tons for 2 min and the spectrum was taken in the range of 400 to 4 000 cm^{-1} with resolution 4 and 128 times scanning.

X-ray Photoelectron Spectroscopy (XPS) is one of the most important techniques for the study of the evidence for successful doping of Eu^{+3} in Eu:HAp. It can be said that the surface sensitivity (typically 40–100 Å) makes this technique ideal for measurements as oxidation states or biomaterials powder. In this analysis we have used a VG ESCA 3 MK II XPS installation ($E_{k\alpha}$ = 1 486.7 eV). The vacuum analysis chamber pressure was $p \sim 3\times10^{-8}$torr. The XPS recorded spectrum involved an energy window w = 20 eV with the resolution R = 50 eV with 256 recording channels. The XPS spectra were processed using Spectral Data Processor v 2.3 (SDP) software.

3. RESULTS AND DISCUSSIONS

Figure 1 shows the XRD patterns of pure HAp (A) and EuHAp (B) with Eu/(Ca+Eu)=20%. Figure 1 (A) shows the typical diffraction peaks of hexagonal $Ca_{10}(PO_4)_6(OH)_2$ for each sample (ICDD file no. 9-432, for instance). No other crystalline phases were detected beside this (phase). The determination of the average crystallite size by XRD method is based on the Scherrer equation: $D_{crystallite} = K\lambda/B\cos\theta$, where $D_{crystallite}$ is the averaged length of coherence domains (that is of perfectly ordered crystalline domains) taken in the direction normal to the lattice plane that corresponds to the diffraction line (00l) taken into account, B is the line broadening due to the small crystallite size, λ is the wavelength of X-rays, θ is the Bragg angle, and K a constant related to crystallite shape and to the definition of B (integral breadth or full width at half maximum). The following results were obtained for the mean crystallite size: D = 18 nm (±0.1) for pure HAp and D = 12 nm (±0.5) nm for EuHAp with Eu/(Ca+Eu) = 20%. As the Eu concentration increases

to 20% the peaks broaden and the mean crystallite size decrease, suggesting that the doping inhibits the HAp crystal growth and/or causes lattice perturbations (microstrain).

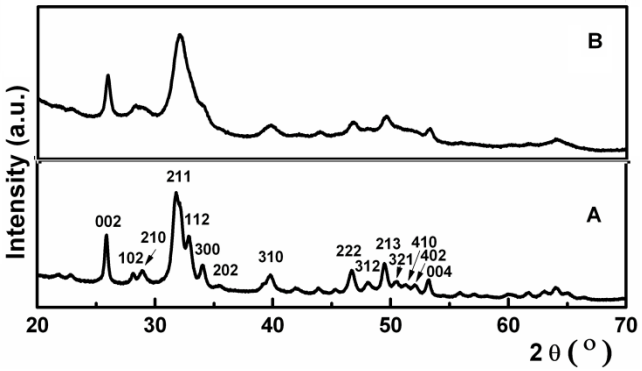

Fig. 1 – The XRD patterns of HAp and Eu:HAp samples synthesized with Eu/(Ca+Eu) = 20% (ICDD-PDF no. 9-432).

Figure 2 presents TEM micrograph (left) of the EuHAp nano-cristallytes with low resolution. Figure 2 (right) shows Selected Areas Electron Diffraction (SAED) pattern of the synthesized powder, which confirm its crystallinity. As shown in Fig. 2, the sample EuHAp exhibits an ellipsoidal morphology which is consistent with the SEM results.

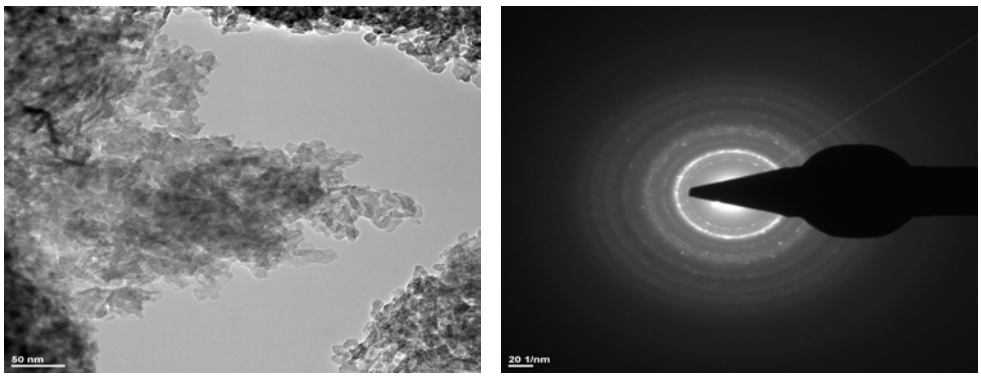

Fig. 2 – TEM images and SAD micrograph of the Eu:HAp (Eu/[Ca+Eu]=20%) samples.

The SEM images of EuHAp samples prepared by co-precipitation are displayed in Fig. 3 SEM images provide the direct information about the size and morphology of the prepared samples. It is found that the EuHAp sample consist of relatively uniform ellipsoidal particles. Figure 3 shows the phase maps based on selected region of the sample EuHAp and simultaneous distributions of individual

elements (Ca, P, Eu). In Fig. 3 the mapping region studied show a uniform of constituent elements, which reveals a homogeneous aspect of the synthesized particles for the sample.

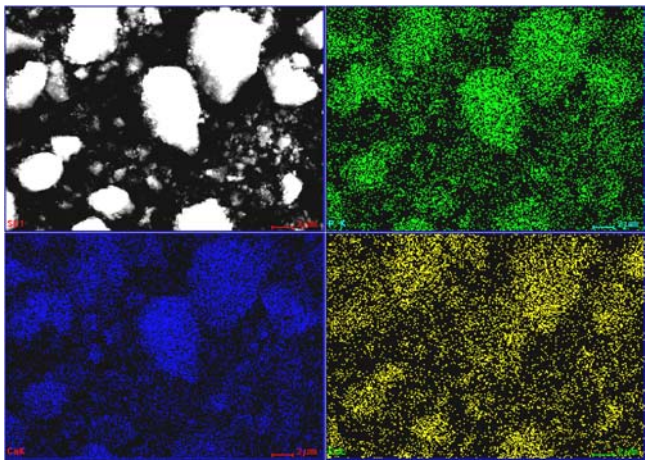

Fig. 3 – The phase maps based on selected region of the sample EuHAp with simultaneous distributions of individual elements (Eu/[Ca+Eu]=20%).

Figure 4 shows the FT-IR results obtained from HAp and EuHAp when the atomic ratio Eu/(Ca+Eu) is equal with 20%. The broad band in the regions 1600-1700 cm^{-1} and 3200-3600 cm^{-1} corresponds to H-O-H bands of lattice water [22-24]. For both samples the bands characteristics of the phosphate and hydrogen phosphate groups in apatite environment were observed: 565 cm^{-1}, 632 cm^{-1}, 603 cm^{-1}, 962 cm^{-1}, and 1000-1100 cm^{-1} for the PO_4^{3-} groups [25] and at 875 cm^{-1} for the HPO_4^{2-} ions. The intensity of vibration peak decreases when the atomic ratio Eu/(Ca+Eu) increases, results those are in good agreement with the XRD analysis.

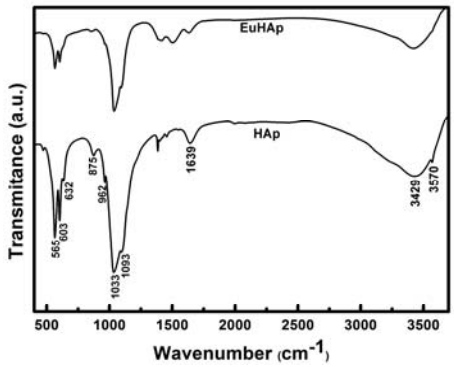

Fig. 4 – The FT-IR results obtained from HAp and EuHAp when the atomic ratio Eu/(Ca+Eu) is equal with 20%.

XPS technique has been tested as a powerful tool for qualitatively determination of surface composition of one material. The XPS spectrum (Fig. 5) of EuHAp is in the binding energy range of 0–1 200 eV.

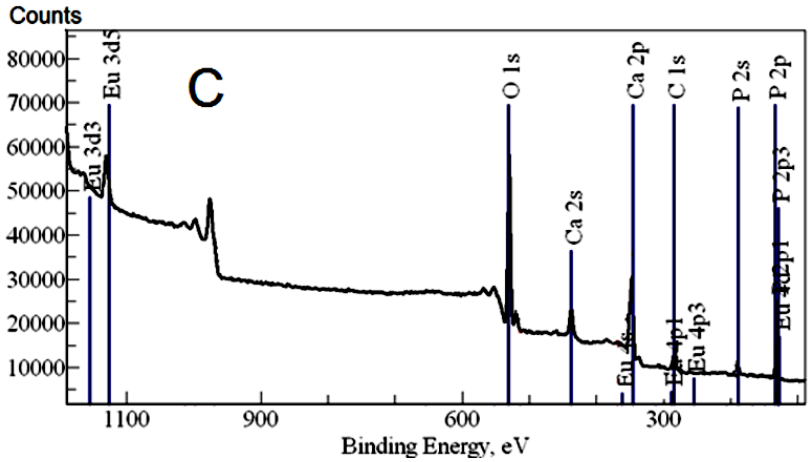

Fig. 5 – XPS spectrum of the EuHAp with Eu/[Ca+Eu]=20%.

The survey XPS spectrum of the sample EuHAp is presented in Fig. 5. Gaussian resolving was performed on Eu 3d5/2, Ca 2p3/2, P 2p3/2, O 1s and C1s spectral lines to investigate the distributing of Eu, Ca, P, O, C elements. (Table 1) The value of binding energy reported in Table 1 for Eu 3d5/2 spectral line show the existence of an oxide (Eu_2O_3).

Table 1

The distribution of Eu, Ca, P, O, C

Spectral line	Binding energy (eV)
C 1s	284.7
O 1s	531.0
Ca 2p3/2	347.1
P 2p3/2	133.8
Eu 3d5/2	1135.2

4. CONCLUSIONS

The europium-doped HAp were synthesized at 80°C by co-precipitating from a mixture of Ca^{2+} and Eu^{3+} ions by phosphate ions in water medium. The preliminary XRD studies have shown that Eu^{3+} has been successfully doped into HAp and no other crystalline phases were detected beside this (hydroxyapatite phase). The as-prepared EuHAp samples conserve regular ellipsoidal morphology

and are homogenous. The XRD, TEM, SEM and FTIR preliminary results are consistent one with another and show that hydroxyapatite could be used in the environment field due to specific physico-chemical properties that allow embedding of Eu^{3+} (Eu^{3+} substitute calcium from the structure of hydroxyapatite) in his structure, without major changing of the structure.

Acknowledgements. The authors would like to acknowledge dr. D. Predoi for his constructive discussions for experimental analysis. Work on this paper has been supported by project: POSDRU/88/1.5/S/56668, ID 56668 Invest in people! European Social Fund, Human Resources Development Operational Programme 2007–2013, Priority axis 1 – "Education and training in support of growth and development of knowledge-based society." I would hereby like to express my full appreciation and gratitude for all your support.

REFERENCES

1. K.E. Uhrich *et al.*, Che. Rev., **99**, 3181 (1999).
2. T. Chandy *et al.*, Biomaterials, **17**, 61 (1996).
3. R. Cortesi *et al.*, Biomaterials, *19*, 1641 (1998).
4. M.A. Rauschmann *et al.*, Biomaterials, **26**, 2677 (2005).
5. E. Esposito *et al.*, Biomaterials, **17**, 2000 (1966).
6. C. S. Ciobanu *et al.*, Optoelectron. Adv. Mater.-Rapid Commun., **4**, 1515 (2010).
7. L. Applegate, *Membrane Separation Processes*, Chem. Eng., **91**, 64 (1984).
8. K. Sengupta *et al.*, Wat. Res., **20**, *9*, 1177 (1986).
9. M. Erdem *et al.*, J. Haz. Mat., **113**, 217 (2004).
10. R. Ternane *et al.*, Opt. Mater., **16**, 291 (2001).
11. A. Doat *et al.*, Biomaterials, **24**, 3365 (2003).
12. A. Doat et al., A. Lebugle, J. Solid State Chem., **178**, 2354 (2005).
13. A. Doat *et al.*, J. Solid State Chem., **177**, 1179 (2004).
14. D. Predoi *et al.*, M. Costache, J. Optoelectron. Adv. Mater., **9**, *12*, 3827 (2007).
154. I. V. Popescu *et al.*, Rom. J. Phys., **55**, 821 (2010).
16. A. Ene *et al.*, Rom. J. Phys., **55**, 806(2010).
17. V. Cuculeanu *et al.*, Rom. Rep. Phys., **62**, 383 (2010).
18. C. G. Popescu, Rom. Rep. Phys., **63**, 471 (2011).
19. G. Rusu-Zagar *et al.*, Rom. Rep. Phys., **63**, 196 (2011).
20. G. State *et al.*, Rom. J. Phys., **56**, 240 (2011).
21. C. Stihi *et al.*, Rom. J. Phys., **56**, 257 (2011).
22. D. Predoi *et al.*, J. Optoelectron. Adv. Mater., **9**, *11*, 3609 (2007).
23. A. Costescu *et al.*, Dig. J. Nanomater. Biostruct., **5**, 989 (2010).
24. C. S. Ciobanu *et al.*, Optoelectron. Adv. Mater.-Rapid Commun., **4**, 1515 (2010).
25. J. Elliot, *Structural and Chemistry of Apatites and other Calcium Ortophosphates*, Elsevier, Amsterdam, 1994.